Supporting Information

Engineering the electronic structure of sub-nanometric Ru clusters via Pt single-atoms modified for high-efficient electrocatalytic hydrogen evolution

Author list has been anonymized.

[a] Address

[b] Address

E-mail:

Contents:

1. Materials and Instrumentation

All reagents used in the syntheses were commercially available and used without further purification. Powder X-ray diffraction (PXRD) was performed with a Rigaku D/MAX2550 diffractometer. Scanning electron microscopy (SEM) was performed on JSM-7500F. Transmission electron microscopy (TEM) was performed on FEI Tecnai G2 S-Twin with a field emission gun operating at 200 kV. Images were acquired digitally on a Gantan multiple CCD camera. Energy dispersive spectroscopy (EDS) spectra were obtained using a JEOL JSM-6300 at 5 kV. Inductively coupled plasma-optical emission spectrometry (ICP-OES) was carried out on an Agilent 730. X-ray photoelectron spectroscopy (XPS) measurements were performed on an ESCALAB 250 X-ray photoelectron spectroscopy, using Mg Kα X-ray as the excitation source. The X-ray absorption data were recorded at beam line BL14W1 of the Shanghai Synchrotron Radiation Facility (SSRF), China.[1]

2. Synthetic Procedures

2.1 Synthesis of CNT-NPA

PA (1.4 mL) was diluted in H_2O (24 mL) to form a clear solution. Then, CNT-NH_2 (50 mg) was added to the mixture. The mixture was dispersed by ultrasonication at room temperature for 1 h and then reacted in an oven at 100 °C for 12 h. After cooling, the resulting sample was washed several times with H_2O and dried at 60 °C for further use.

2.2 Synthesis of CNT-NPA-PtRu

The as prepared CNT-NPA was dispersed in mixed solution including 2.9 mL of H_2O, 300 μL of $RuCl_3$ aqueous solution (10 mg mL^{-1}), and 120 μL of $PtCl_4$ aqueous solution (10 mg mL^{-1}) by ultrasonication at room temperature for 1 h. The mixture was stirred at 50 °C for 18 h and then separated by centrifugation, washed with deionized water and methanol. The CNT-NPA-PtRu was finally obtained after drying overnight in a vacuum oven at 60 °C.

2.3 Synthesis of CNT-NPA-Ru and CNT-NPA-Pt

As control samples, monometallic catalysts, CNT-NPA-Ru and CNT-NPA-Pt, were synthesized following the same procedure with only $RuCl_3$ or $PtCl_4$ used in the CNT-NPA-PtRu process.

2.4 Synthesis of CNT-N-PtRu

The CNT-NH_2 (50 mg) was dispersed in mixed solution including 2.9 mL of H_2O, 300 μL of $RuCl_3$ aqueous solution (10 mg mL^{-1}), and 120 μL of $PtCl_4$ aqueous solution (10 mg mL^{-1}) by ultrasonication at room temperature for 1 h. The mixture was stirred at 50 °C for 18 h and then separated by centrifugation, washed with deionized water and methanol. The CNT-NPA-PtRu was finally obtained after drying overnight in a vacuum oven at 60 °C.

2.5 Synthesis of CNT-CPA-PtRu and CNT-OPA-PtRu

The synthetic process is similar with the CNT-NPA-PtRu, except for using CNT-COOH and CNT-OH as substrate material.

2.6 Synthesis of CNT-NPA-PtRu-n_1

The as prepared CNT-NPA was dispersed in mixed solution including 2.9 mL of H_2O, 600 μL of $RuCl_3$ aqueous solution (10 mg mL^{-1}), and 240 μL of $PtCl_4$ aqueous solution (10 mg mL^{-1}) by ultrasonication at room temperature for 1 h. The mixture was stirred at 50 °C for 18 h and then separated by centrifugation, washed with deionized water and methanol. The CNT-NPA-PtRu-n_1 was finally obtained after drying overnight in a vacuum oven at 60 °C.

2.7 Synthesis of CNT-NPA-PtRu-n_2

The as prepared CNT-NPA was dispersed in mixed solution including 2.9 mL of H_2O, 900 μL of $RuCl_3$ aqueous solution (10 mg mL^{-1}), and 360 μL of $PtCl_4$ aqueous solution (10 mg mL^{-1}) by ultrasonication at room temperature for 1 h. The mixture was stirred at 50 °C for 18 h and then separated by centrifugation, washed with deionized water and methanol. The CNT-NPA-PtRu-n_2 was finally obtained after drying overnight in a vacuum oven at 60 °C.

3. Characterization

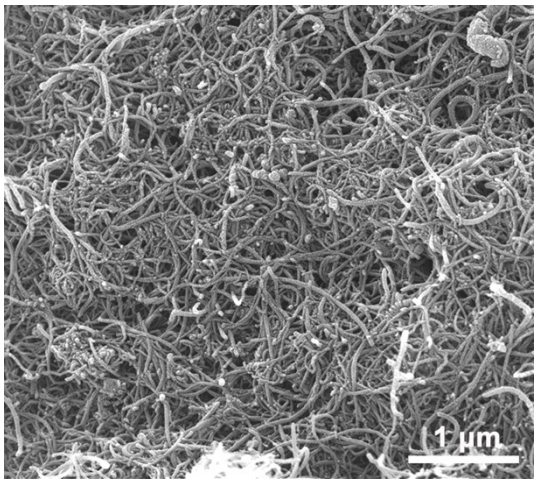

Figure S1. SEM image of CNT-NPA-PtRu.

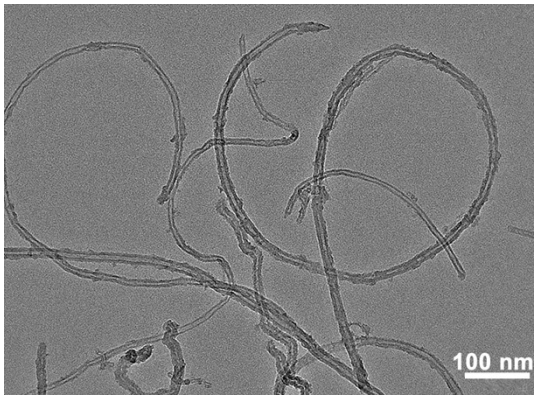

Figure S2. TEM image of CNT-NPA-PtRu.

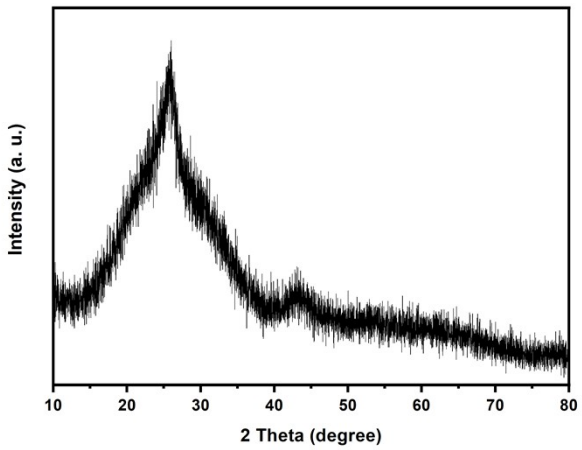

Figure S3. Power XRD pattern of CNT-NPA-PtRu.

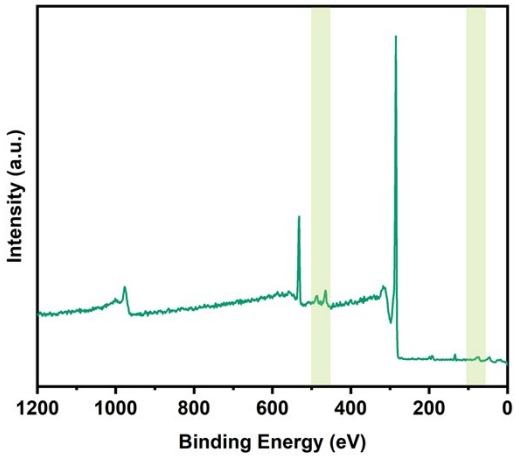

Figure S4. XPS spectra of CNT-NPA-PtRu.

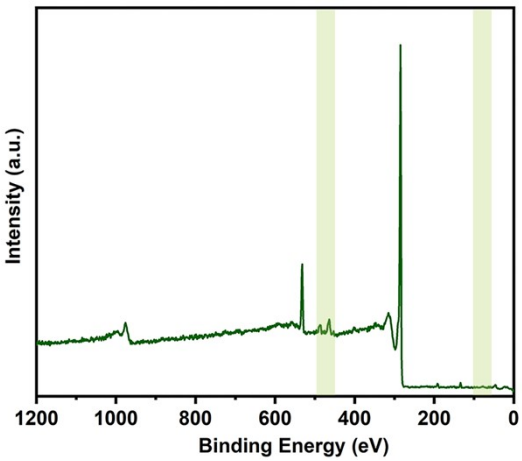

Figure S5. XPS spectra of CNT-NPA-Ru.

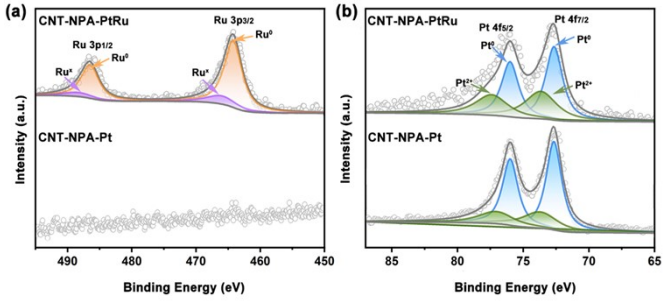

Figure S6. The XPS spectra of CNT-NPA-PtRu and CNT-NPA-Pt for (a) Ru 3p and (b) Pt 4f.

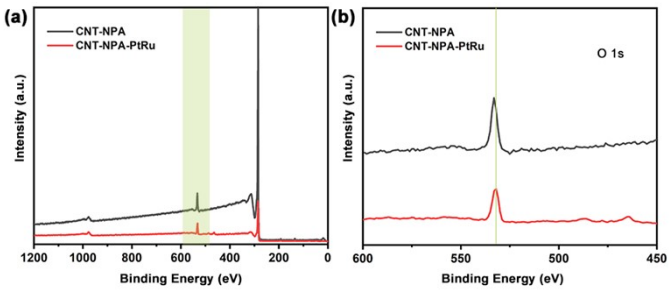

Figure S7. XPS spectra of CNT-NPA and CNT-NPA-PtRu.

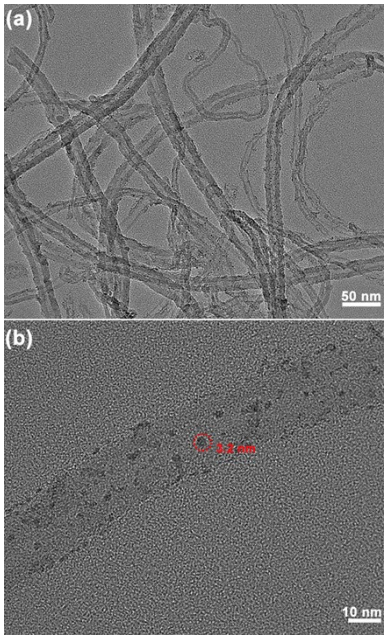

Figure S8. TEM images of CNT-N-PtRu.

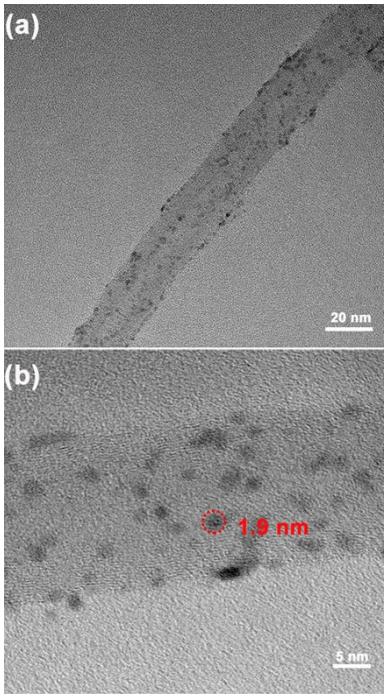

Figure S9. TEM images of CNT-NPA-PtRu-n_1.

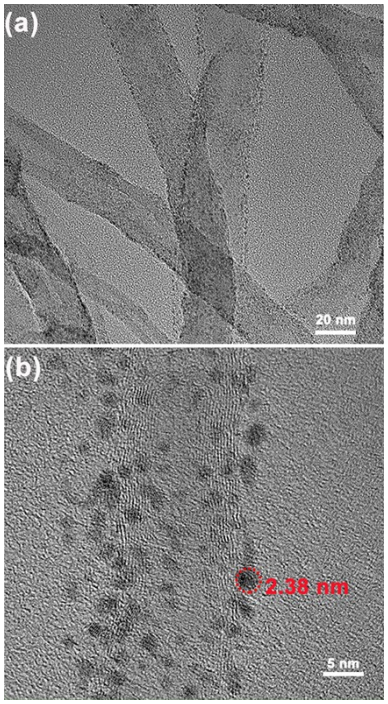

Figure S10. TEM images of CNT-NPA-PtRu-n_2.

4. Electrochemical measurements

All electrochemical tests were measured on an electrochemical work station (CHI760E Shanghai, Chenhua) with representative three-electrode configuration. A polished glassy carbon electrode was used as the working electrode (3 mm diameter, 0.07065 cm^2), a graphite rod electrode was served as the counter electrode and the saturated calomel electrode (SCE) acted as the reference electrode. The ink used in the test was prepared by mixing 5 mg of catalyst with 400 μL water, 600 μL ethanol, and 20 μL 5 wt% Nafion under ultrasound for 0.5 h. Then 5 μL catalyst ink was dropped on the glassy carbon electrode, and the catalyst loading on the electrode was 0.34 mg cm^{-2}. Next, test the activity at different pH values in 1 M KOH, 0.5 M H_2SO_4, and 1 M PBS solutions. Linear sweep voltammetry (LSV) was performed at a scanning speed of 5 mV s^{-1}, with a voltage range of -1 to -1.7 V in 1 M KOH, -0.2 to -1 V in 0.5 M H_2SO_4, and -0.5 to -1.6 V in 1 M PBS. The durability of the catalyst was measured using chronoamperometry. Electrochemical impedance (EIS) is tested in the frequency range of 100 kHz to 0.01 Hz. The electrochemical active surface area (ECSA) of the electrocatalyst was measured by double-layer capacitance (C_{dl}), and its values can be obtained by cyclic voltammetry at different scanning rates of 20, 40, 60, 80, 100, and 120 mV s^{-1}.

Measurement of the turnover frequency (TOF). TOF was calculated by the following formula:

$$TOF\ (s^{-1}) = I/(z*n*F)$$

where I is the current (A) during LSV, F is the Faraday constant (96,485 C mol^{-1}), n is the number of active sites (mol), z is the number of electron transfers in the catalytic reaction, and for HER, the value of z is 2.[2]

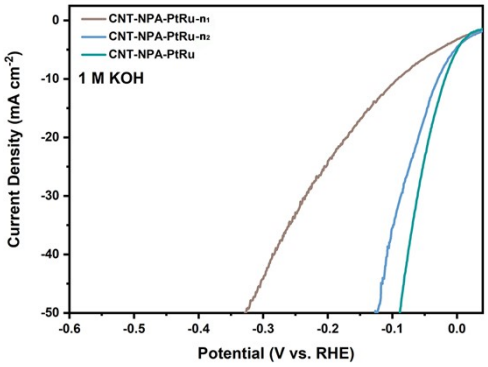

Figure S11. HER LSV curves for CNT-NPA-PtRu-n_1, CNT-NPA-PtRu-n_2, and CNT-NPA-PtRu catalyst in 1 M KOH.

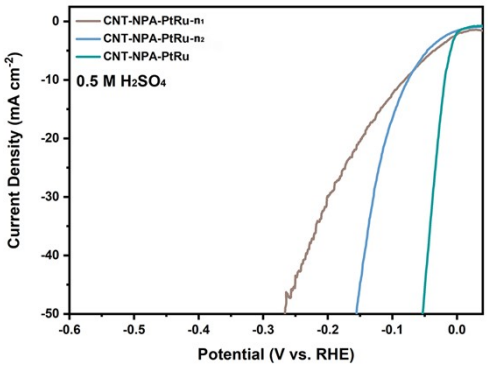

Figure S12. HER LSV curves for CNT-NPA-PtRu-n_1, CNT-NPA-PtRu-n_2, and CNT-NPA-PtRu catalyst in 0.5 M H_2SO_4.

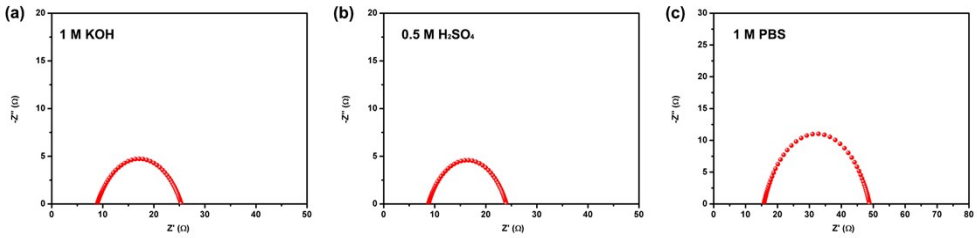

Figure S13. The EIS of CNT-NPA-PtRu in all pH solutions.

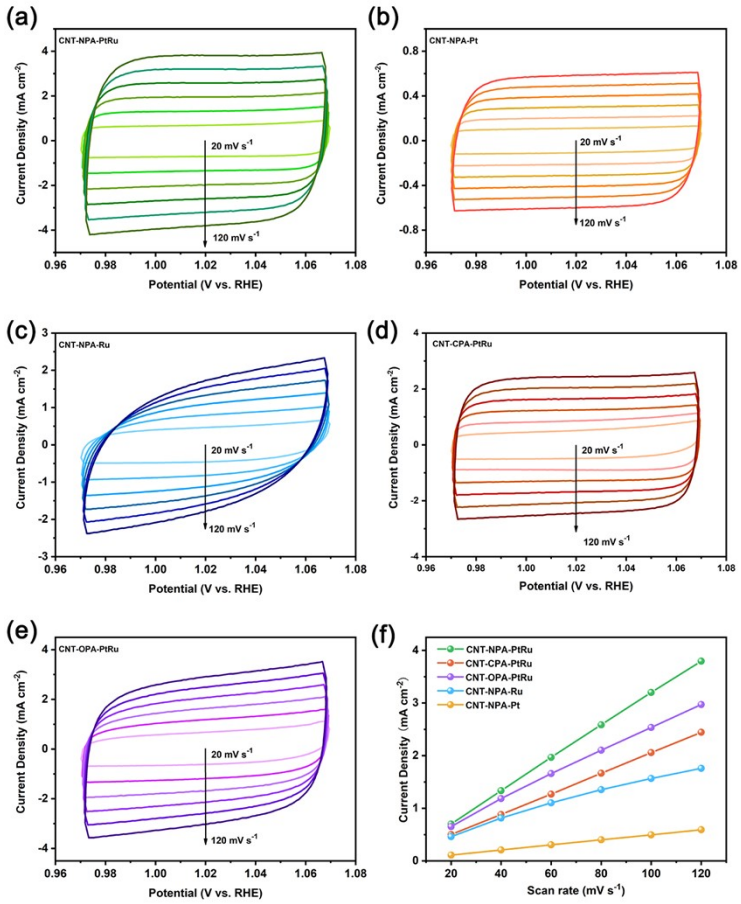

Figure S14. CV curves and C_{dl} values of CNT-NPA-PtRu and different contrast electrocatalysts during HER process in 1 M KOH solution.

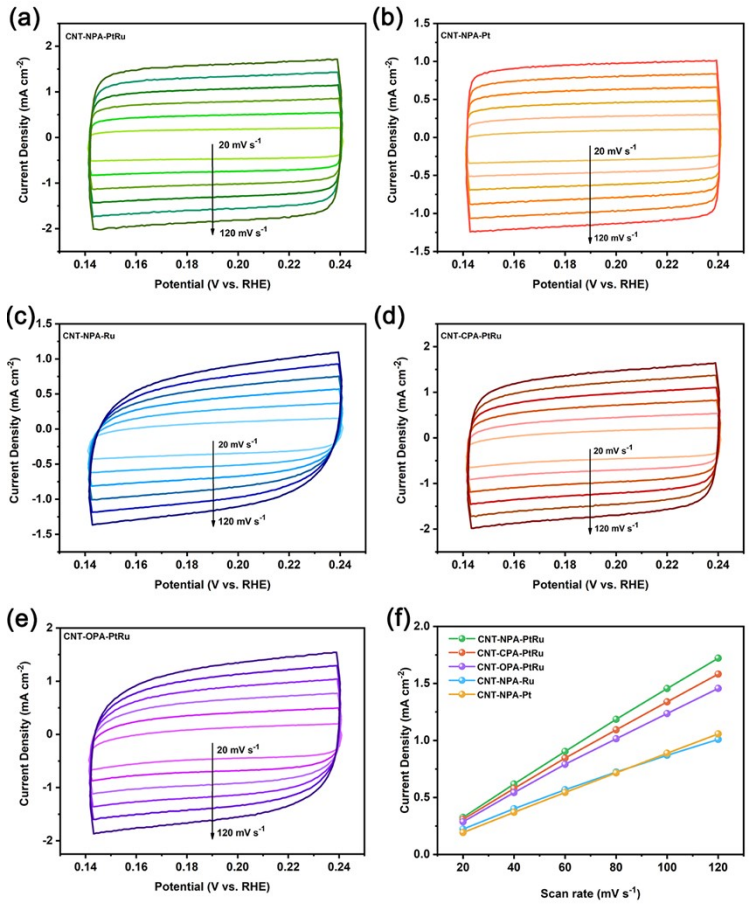

Figure S15. CV curves and C_{dl} values of CNT-NPA-PtRu and different contrast electrocatalysts during HER process in 0.5 M H_2SO_4 solution.

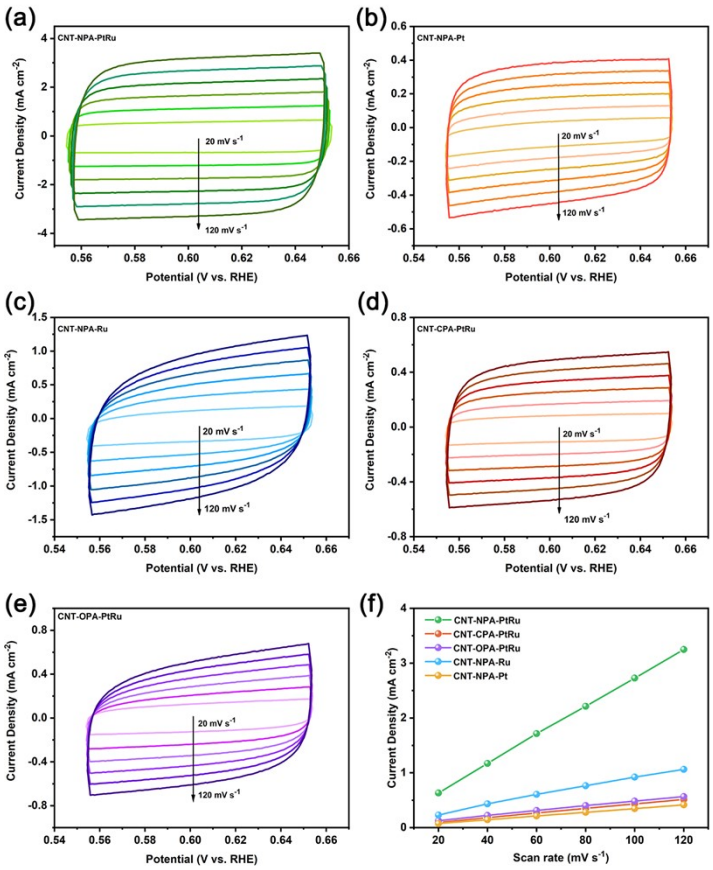

Figure S16. CV curves and C_{dl} values of CNT-NPA-PtRu and different contrast electrocatalysts during HER process in 1 M PBS solution.

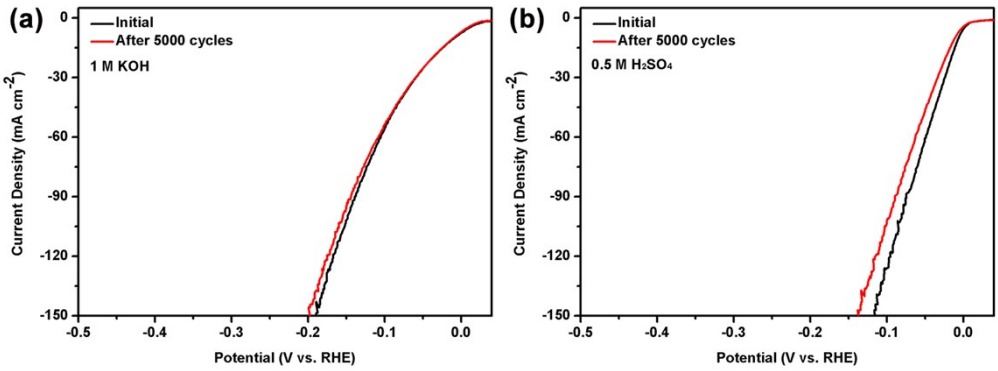

Figure S17. Long-term CV measurement of CNT-NPA-PtRu in 1 M KOH solution (a) and 0.5 M H_2SO_4 solution (b).

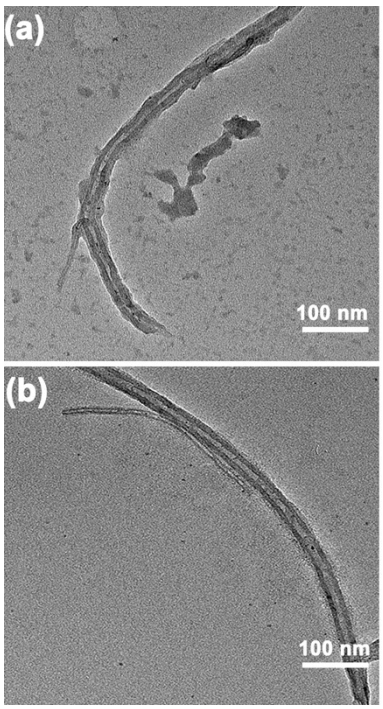

Figure S18. TEM images of CNT-NPA-PtRu after HER cycles in 1 M KOH solution (a) and 0.5 M H_2SO_4 solution (b).

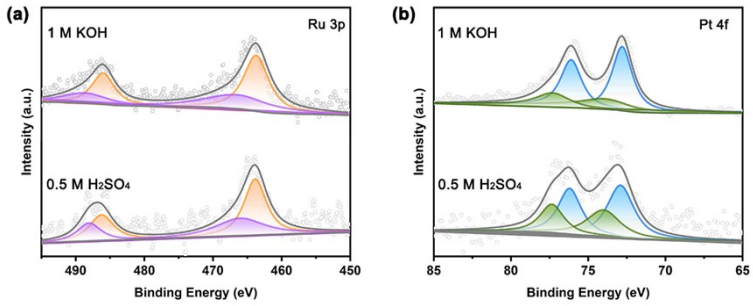

Figure S19. Ru 3p and Pt 4f XPS spectras for CNT-NPA-PtRu after HER cycles.

Table S1. The ICP results of CNT-NPA-PtRu

	Ru	Pt
Comtent (wt%)	6.51	0.60

Table S2. Comparison of reported HER activities for various Ru-based and Pt-based electrocatalysts.

Catalyst	$\eta_{j=10\ mAcm^{-2}}$ (mV)			Reference
	1 M KOH	0.5 M H_2SO_4	1 M PBS	
CNT-NPA-PtRu	18.3	18.7	15	**This work**
RuNi/CQDs	13	58	18	**Angew. Chem. Int. Ed.** 2020, 59, 1718
Ru/OMSNNC	13	27	70	**Adv. Mater.** 2021, 33, 2006965
Mo_2C-Ru/C	22	64	37	**Adv. Funct. Mater.** 2023, 2301925
PtCo@PtSn	25	21	18	**Adv. Funct. Mater.** 2021, 2107597
MI-PtZnCo	29	20	48.3	**Adv. Energy Mater.** 2022, 2201478
Ru SAs-Ni_2P	57	125	260	**Nano Energy** 2021, 80, 105467
Ru_2B_3@BNC	7	41	58	**Nano Energy** 2020, 75, 104881
Co_5Ru_1@NCNT/PF	28	45	28	**Adv. Sci.** 2022, 9, 2200010
Ru/HMCs-500	26.93	48.09	74.16	**J. Mater. Chem. A** 2023, 11, 3524
PtRu/CC_{1500}	19	8	25	**J. Mater. Chem. A** 2020, 8, 2090
HP-Ru/C	25	38	52	**Appl. Catal. B Environ.** 2021, 294, 120230
$Ru_{0.10}$@2H-MoS_2	51	168	137	**Appl. Catal. B Environ.** 2021, 298, 120490
Ni_2P-Ru_2P/CCG-800	21.83	49.42	113.38	**Chem. Eng. J.** 2022, 432, 134422
Ru-CB[6]/MWCNTs	27	37	70	**Chin. Chem. Lett.** 2023, 34, 107717
PtRu/CC-P	44	42	41	**Nanoscale** 2022, 14, 15942
Ru NCs/NC	14	32	30	**Nano Res.** 2023, 16, 9073
Ru/RuO_2	17	16	29 (1 M KPi)	**Energy Environ. Sci.** 2021, 14, 5433
Ru/Co@NC	10	50	283 (0.01 M PBS)	**Chem. Eng. J.** 2022, 450, 138254

Ru_1CoP/CDs	51	49	-	**Angew. Chem. Int. Ed.** 2021, 60, 7234
Ru_{1+NPs}/N−C	39	75	-	**ACS Appl. Mater. Interfaces** 2022, 14, 15250
fcc-RuCu HUNSs	26	25	-	**Sci. China Chem.** 2022, 65, 87
Pt-PdO/C	29	16	-	**ACS Sustainable Chem. Eng.** 2022, 10, 37
Pd-Ru@NG	28	39	-	**Chem. Commun.** 2019, 55, 13928

5. Theoretical calculation

Spin-polarized DFT calculations were performed using the Vienna ab initio simulation package (VASP). [3,4] The generalized gradient approximation proposed by Perdew, Burke, and Ernzerhof (GGA-PBE) is selected for the exchange-correlation potential.[5] The pseudo-potential was described by the projector-augmented-wave (PAW) method.[6] The geometry optimization is performed until the Hellmann-Feynman force on each atom is smaller than 0.02 eV·Å^{-1}. The energy criterion is set to 10^{-6} eV in iterative solution of the Kohn-Sham equation.

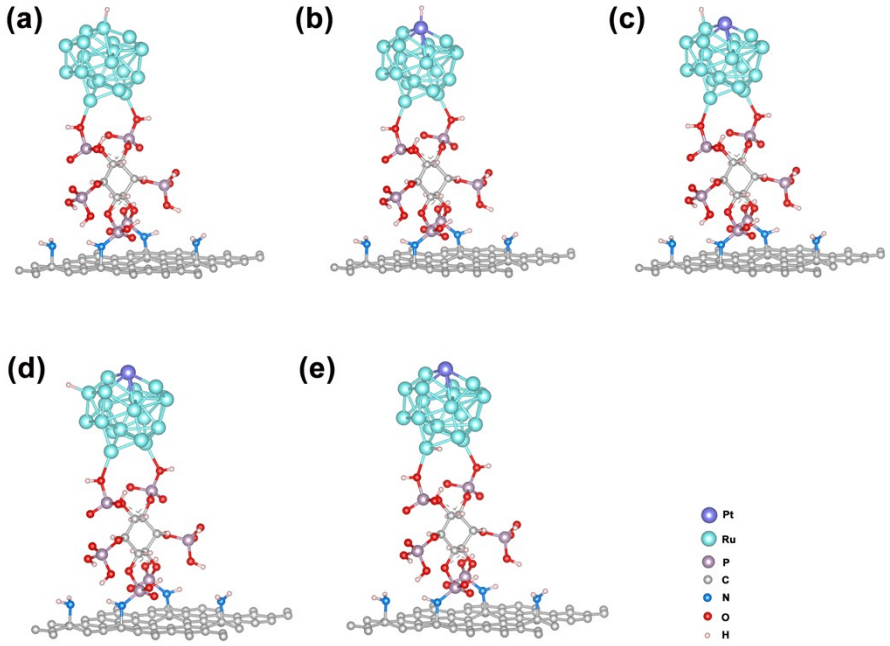

Figure S20. The side view of chemisorption models of H* on Ru@CNPA-Ru (a), Pt@CNPA-PtRu (b), Ru_1@CNPA-PtRu (c), Ru_2@CNPA-PtRu (d), and Ru_3@CNPA-PtRu (e).

Table S3. The ΔG_{H^*} value of different Ru sites of CNPA-Ru and CNPA-PtRu

	Ru@CNPA-Ru	Pt@CNPA-PtRu	Ru_1@CNPA-PtRu	Ru_2@CNPA-PtRu	Ru_3@CNPA-PtRu
ΔG_{H^*} (eV)	-0.577	-0.414	-0.482	-0.571	-0.601

References

[1] H. S. Yu, X. J. Wei, J. Li, S. Q. Gu, S. Zhang, L. H. Wang, J. Y. Ma, L. N. Li, Q. Gao, R. Si, F. F. Sun, Y. Wang, F. Song, H. J. Xu, X. H. Yu, Y. Zou, J. Q. Wang, Z. Jiang and Y. Y. Huang, *Nucl. Sci. Tech*., 2015, **26**, 50102. The authors thank beamline BL14W1 (Shanghai Synchrotron Radiation Facility) for providing the beam time.

[2] R. Zhang, Y. Li, X. Zhou, A. Yu, Q. Huang, T. Xu, L. Zhu, P. Peng, S. Song, L. Echegoyen and F. F. Li, *Nat. Commun*., 2023, **14**, 2460.

[3] G. Kresse and J. Furthmüller, *Comput. Mater. Sci*., 1996, **6**, 15-50.

[4] G. Kresse and J. Furthmüller, *Phys. Rev. B*, 1996, **54**, 11169-11186.

[5] J. P. Perdew, K. Burke and M. Ernzerhof, *Phys. Rev. Lett*., 1996, **77**, 3865-3868.

[6] P. E. Blöchl, *Phys. Rev. B*, 1994, **50**, 17953-17979.